Int. J. Solids Structures Vol. 29, No. 14/15, pp. 1753–1761, 1992
Printed in Great Britain.
0020-7683/92 $5.00 + .00
Pergamon Press plc

MICROBUCKLING AND STRENGTH IN LONG-FIBER COMPOSITES: THEORY AND EXPERIMENTS

J.-C. GRANDIDIER, G. FERRON and M. POTIER-FERRY
Laboratoire de Physique et de Mécanique des Matériaux, U.R.A. C.N.R.S. 1215,
Institut Supérieur de Génie Mécanique et Productique, Ile du Saulcy, F 57045 Metz Cedex 01

Abstract—Failure of laminated composites in compression is often ascribed to a mechanism of fiber microbuckling. Following this interpretation, a model is presented where the fiber is schematized as an elastic beam and the matrix as an elastic foundation. In comparison with previous models, however, the strain in the matrix is distributed through the thickness of a ply and lower failure stresses are obtained. An original flexion–compression device designed for investigating the elastic behavior in compression and the effect of the loading mode on the characteristics of failure is then described. Results on glass/epoxy resin unidirectional composites and laminates are discussed.

1. INTRODUCTION

The mechanical performance of long-fiber composite materials and structures has significantly been improved in recent years. These advances are the result of a better understanding of their behavior together with an increase in the mechanical properties of the basic products and improvements in manufacturing techniques. For instance, the tensile stiffness of graphite fibers was about 150 GPa when they were first put on the market, and it may attain 500 GPa at this time. Their tensile strength also has been increased. The effect of these improvements on the tensile properties of laminates is manifest. This is not true, at least to the same extent, with regard to their behavior in compression.

In this paper, the differences between the tensile and compressive behaviors of laminates are first outlined, and the microbuckling models developed in the literature to account for failure in compression are briefly recalled. Following previous authors a microbuckling model is then presented, where the behavior of a family of fibers in the thickness of a ply is considered. Finally, a new flexion–compression device is described, and the results relating to the effect of the loading mode on the elastic behavior and on the characteristics of failure are discussed.

2. EXPERIMENTAL AND THEORETICAL ASPECTS OF THE COMPRESSIVE BEHAVIOR OF LAMINATES

Two main kinds of tests are usually performed to estimate the compressive behavior of composites: compression tests and pure flexion tests. In spite of the difficulties which are inherent in the compression tests, it seems well established that both the stiffness and the strength of long-fiber composites are lower in compression than in tension. For instance, Stevanovic and Nesic (1987), using the Celanese test (ASTM D3410), measured on T300/108 graphite/epoxy resin unidirectional composites a stress at failure equal to 1225 MPa in compression. This value is to be compared with that obtained in tension, 1562 MPa. They also noted a decrease in stiffness during compressive loading, with a value of Young's modulus of 112 GPa for 0.3% strain instead of 139 GPa in tension.

Recently, a sophisticated four-points flexion device was set up by Vittecoq (1991) (see also Allix *et al.*, 1988). The laminates tested were made of T300/914 and IM6/914 graphite/epoxy resin pre-impregnated tapes. The evolution, as a function of the bending moment, of the strains measured on the two faces under tension and under compression shows that the tensile behavior is almost linear and that the compressive behavior is non-linear. The loss of stiffness observed in compression starts from the onset of loading, and steadily increases during the test. This behavior is macroscopically elastic, as was confirmed by a series of loadings and unloadings. The non-linear response of the laminates depends on the stacking sequence of the plies and on the type of fibers utilized. In particular, the loss of stiffness increases when the fiber diameter is decreased. When comparing pure flexion and compression tests, Vittecoq (1991) also observed that the stresses at failure are lower, but that the corresponding strains are higher in flexion than in compression.

Summarizing, it clearly appears that both the stiffness and the strength are lower in compression than in tension. In addition these characteristics depend on the stacking sequence, on the fibers utilized and on the mode of loading.

The lower stiffness in compression may consistently be associated with geometric non-linearities. The scale at which these non-linearities take place is an open question. They may occur at the scale of the fibers: as shown by Greenwood and Rose (1974) a Kevlar fiber under bending is capable of developing a bulge on its surface. The authors explained this behavior by variations in hardness along the radius of the fiber. As a result of the lower hardness of the core of the fiber, it would behave much in the same way as a thin cylinder of high slenderness. The non-linearities may also develop at the scale of few fibers. As discussed below, this behavior has been observed experimentally in pure flexion tests, on the face under compression. Finally the non-linearities may occur at the scale of the width of a strand. This characteristic dimension of the initial product is frequently considered as critical in the mechanisms of damage.

The lower strength in compression is often ascribed to some instability of the composite, such as a process of microbuckling at the scale of a few fibers. The first model of microbuckling was developed by Rosen (1964; see also Kulkarni et al., 1975). The composite is schematized as a superimposition of hard and soft layers representing the fibers and the matrix. Under a compressive load parallel to the direction of the layers, two modes of instability may occur. One is an in-phase mode, the other an out-of-phase mode. The matrix is then submitted either to shearing or to tension–compression, respectively. The critical stress is determined by modeling the hard layer as a beam on foundations. For volume fractions of fibers larger than 0.25 the in-phase mode is operative. Then, the critical stress is found to be equal to:

$$\sigma_c = \frac{G_M}{(1-f)}$$

where G_M is the shear modulus of the matrix and f is the volume fraction of fibers. As a first approximation, this critical stress is equal to the global shear modulus in the plane of the fibers. When this result is applied to graphite/epoxy resin composites, this stress is much higher than the experimental failure stress. Several models (Hanasaki and Hasegawa, 1974; Davis, 1975; Greszczuk, 1975; Kulkarni et al., 1975; Schaffers, 1976; Greszczuk, 1982; Steif, 1987, 1988; Harris and Lee, 1988; Anquez, 1990) have been proposed to improve the initial treatment of Rosen (1964). In spite of these efforts the critical stress always remains of order of the shear modulus of the composite. It is therefore not possible to decide whether microbuckling is the controlling process of failure in compression. Moreover, these models do not allow us to account for the effects of the stacking sequence and of the mode of loading (pure flexion or pure compression). An important drawback also comes from the fact that no characteristic microbuckling wavelength is provided by these models.

3. MICROBUCKLING MODEL

In order to overcome the drawbacks mentioned above, a new approach to microbuckling was proposed by Grandidier and Potier-Ferry (1990). In this treatment a family of fibers inside a ply where the stress is compressive in the fiber direction is modeled (Fig.

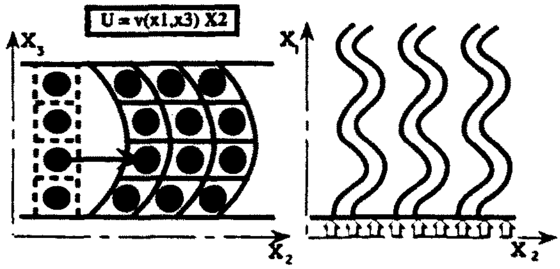

Fig. 1. Displacement assumed in a ply at 0° to the compressive direction x_1; x_2 is the transverse direction parallel to the plies and x_3 is the thickness direction.

1). The fiber displacement is parallel to the faces of the ply and its amplitude depends on the position in the thickness direction. These assumptions allow for the associated shear strain ε_{23} of the matrix to be distributed over a length scale larger than the spacing between fibers. Accordingly, a lower critical stress is expected from this schematization. As a first approximation, the effect of this shearing in the plane normal to the direction of compressive loading has been analysed without considering the other strain components induced by this mode of instability.

With these assumptions the critical stress was estimated by analysing the fiber–matrix association as a beam on foundations. The classical equation for the stability of the beam can be expressed as:

$$E_f I_f \frac{\partial^4 v}{\partial^4 x_1} + \sigma_c S_f \frac{\partial^2 v}{\partial^2 x_1} - F = 0,$$

where E_f is the Young's modulus of the fiber, I_f is its quadratic momentum, S_f is its cross-ssectional area, σ_c is the compressive load applied to the beam and F is the restoring force per unit length produced by the matrix onto the fiber. From dimensional and symmetry considerations this force should be expressed as a function of the displacement v in the following form (Grandidier and Potier-Ferry, 1990):

$$F = CE_M S_f \frac{\partial^2 v}{\partial^2 x_3},$$

where E_M is the Young's modulus of the matrix and C is a non-dimensional coefficient which depends on the volume fraction of fibers and on the Poisson's ratio of the matrix. Coefficient C was determined by computing the microstresses at the interface between the fiber and the matrix. The periodic homogenization theory (Sanchez-Palencia, 1980) was used to solve this problem. Because of the periodicity, the restoring force computed by a development at the first order is zero. The theory was thus carried through at the second order, and the boundary value problems on the unit cell were solved by finite element method calculations.

The solution of the stability equation is then obtained from the knowledge of the boundary conditions imposed on the two faces of the ply. As an illustration, when micro-buckling occurs in an internal ply between two other plies at 90° the displacement is assumed to be zero on the two faces (Fig. 2) and the critical stress can be expressed as:

$$\sigma_c = \sqrt{CE_M E_f}\,\frac{\pi r_f}{t},$$

where t is the ply thickness and r_f is the radius of the fiber. The wavelength is equal to:

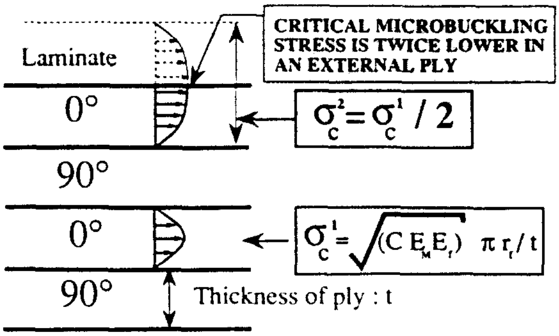

Fig. 2. Influence of boundary conditions on the displacement field and on the critical microbuckling stress, for internal and external plies at 0° to the compressive direction.

$$l = 2\sqrt{\pi}\,\sqrt[4]{\frac{E_{\mathrm{f}}}{CE_{\mathrm{M}}}}\,\sqrt{\frac{I_{\mathrm{f}}t}{S_{\mathrm{f}}}}$$

Alternatively, the condition of free surface should be taken into account for a superficial ply (Fig. 2). In this case the critical stress is twice lower and the wavelength should be divided by $\sqrt{2}$.

With this model, microbuckling is a structural effect which depends on the material and on the stress distribution in the thickness of the laminate. In comparison with previous models, an important improvement comes from the determination of a characteristic wavelength for microbuckling.

A critical strain of 0.39% in a superficial ply is obtained with the model for a 3 mm thick T300/914 graphite/epoxy resin cross-ply laminate with a ply thickness of 0.125 mm. Any quantitative comparison with experiments is nevertheless questionable at this stage. In particular, the effect of the shearing in the (1, 2) plane has so far been disregarded in the analysis. Further refinements of the model should take this effect into account, with a shear strain ε_{12} that should be distributed over a length scale larger than the fiber spacing.

4. FLEXION COMPRESSION DEVICE

An original device has been set up to analyse the behavior of composites under conditions of combined bending and compressive loading. This mechanism was designed in particular to investigate the structural effects relating both to the loading mode and to the stacking sequence of the laminate. The requirements imposed on the design of the device are as follows.

- —The flexion–compression loading of the specimen should be obtained by a mechanical arrangement that converts the uniaxial force of a conventional testing machine into appropriate efforts at the ends of the specimen.
- —Different configurations corresponding to different ratios of bending moment M to compressive load N should be easily workable without complicated handling. In particular, the specimen geometry and the connecting parts between the specimen and the mechanism should be the same for all configurations.
- —For a given configuration, the (M/N) ratio in the central cross-section of the specimen should remain almost constant during the test.

A schematic view of the experimental arrangement is shown on Fig. 3. The mechanism consists of two cantilever beams connected to the tensile testing machine, and of four arms joining the cantilever beams to the connecting parts which transmit the efforts to the specimen.

The evolution of the shape of the mechanism depends on specimen behavior via the relations between bending moment, axial load, rotation and axial displacement at the ends

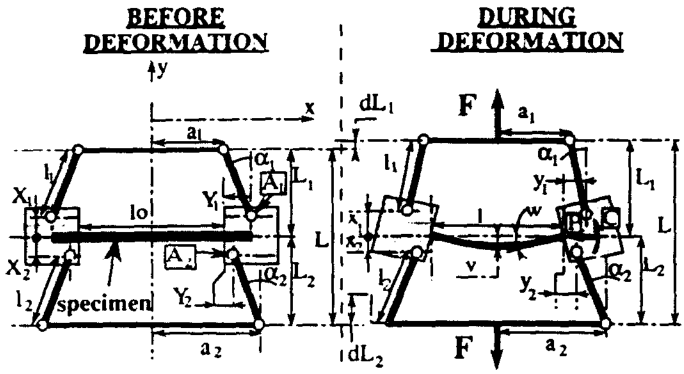

Fig. 3. Principle of the flexion–compression device.

of the specimen. A numerical simulation of the whole arrangement was performed by postulating a linear elastic behavior of the material. Two different assumptions were made concerning specimen deformation. One consists of assuming circular bending, which is appropriate for pure flexion. The other is a small-strain, moderate rotation theory which allows us to account for the non-linear effect of the compressive force. A simple step-by-step computation is performed in the former case, whilst a Newton–Raphson procedure is used in the latter case to solve the non-linear equations of the problem. The (M/N) ratio in the central cross-section of the specimen is also determined at each step of the calculation. The step size in the calculations is taken as the increase in the distance between the two cantilever beams (i.e. the increment of displacement imposed by the testing machine). Three arrangements were adopted. They correspond to three values of the (M/N) ratio in the center of the specimen: -18 mm (Fig. 4); -0.5 mm (Fig. 5) and -1 mm (Fig. 6). The stress distribution in the thickness of the central cross-section of a 3 mm thick specimen is also shown on these figures for a linear elastic behavior of the material.

A fork-joint arrangement was used for the arms between the cantilever beams and the connecting parts in order to transmit efforts in a symmetrical way. Clamping of the specimen was simply assured by means of carefully adjusted slots machined in the connecting parts.

5. EXPERIMENTAL

The behavior of glass/epoxy resin specimens was investigated. Owing to the low stiffness and high strength of glass fibers, microbuckling is consistently expected for this

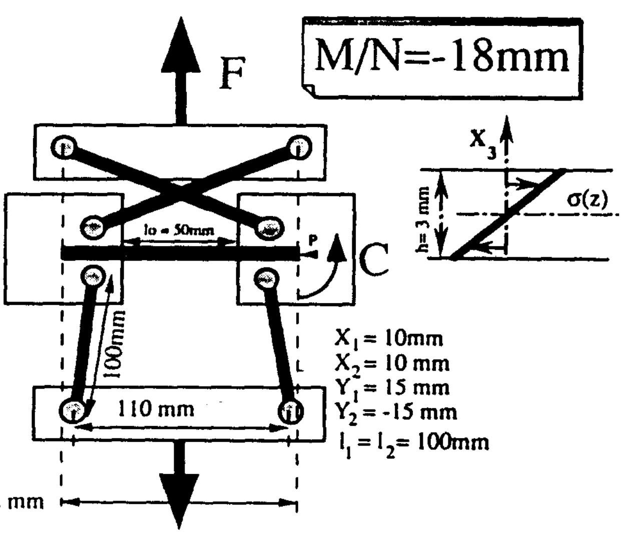

Fig. 4. Dimensions of the device and stress distribution through the thickness for the configuration leading to $M/N = -18$ mm.

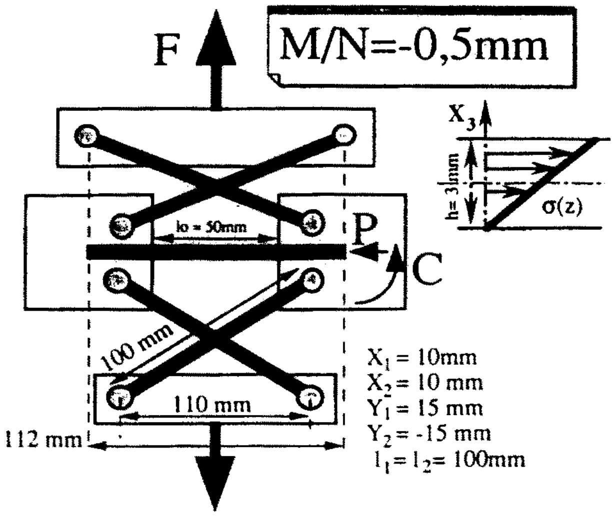

Fig. 5. Dimensions of the device and stress distribution through the thickness for the configuration leading to $M/N = -0.5$ mm.

material, although it may appear only at fairly high strain levels. It is also interesting to compare the behavior of this composite with the results obtained by Vittecoq (1991) on graphite/epoxy resin lamintes under pure flexion.

The basic material was in the form of glass E/epoxy resin preimpregnated tapes which were used to prepare either unidirectional composites (UD) or cross-ply laminated plates which were cut in the form of $[90/0/90/0/90]_S$ and $[0/90/0/90/0]_S$ specimens.

The tests were performed on a screw-driven tensile testing machine with computer facilities. A low, constant cross-head speed was imposed to the mounting. Load and displacement were recorded, together with longitudinal strains obtained from strain-gages located on the upper and lower faces of the specimen.

For the UD specimen and for all the laminates tested under conditions of quasi-pure flexion ($M/N = -18$ mm) the tensile and compressive strains measured on the lower and upper faces are almost equal. The compressive strain actually is slightly higher, due to the fact that a small compressive load is applied to the specimens ($M/N = -18$ mm, to be compared to the thickness of the specimen, ~2.15 mm). These results tend to demonstrate

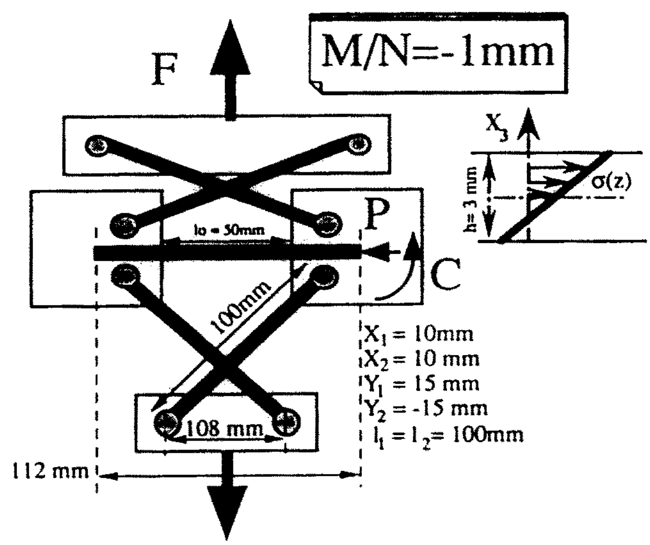

Fig. 6. Dimensions of the device and stress distribution through the thickness for the configuration leading to $M/N = -1$ mm.

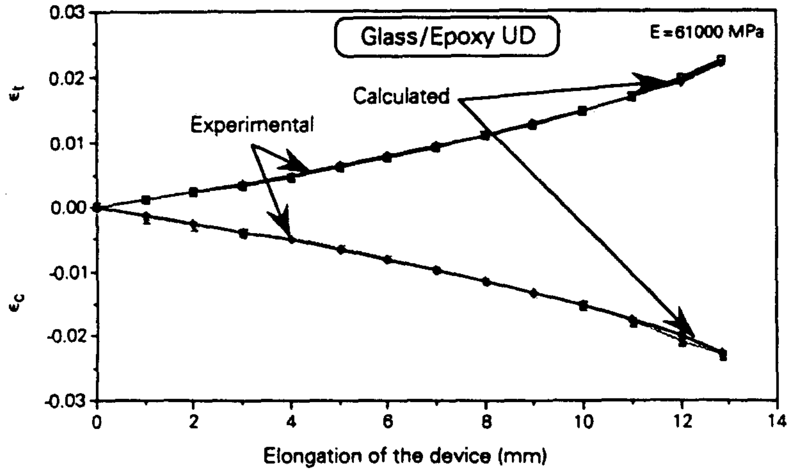

Fig. 7. Experimental and calculated strains on the two faces under tension and under compression for a UD glass/epoxy resin specimen. The calculations are carried out under the assumption of a linear elastic behavior of the material.

that these composites exhibit the same elastic linear behavior both in tension and in compression. The flexion tests were thus simulated by assuming such a behavior and by using the value of Young's modulus obtained from standard tension tests. An excellent correlation between calculations and experiments is obtained for the evolution of strains on the two faces of the specimen (Fig. 7). A further check of the linearity of the behavior in compression is given on Fig. 8, where the experimental and calculated ratios of compressive to tensile strains are plotted as a function of the elongation of the device. On the other hand, the correlation between experimental and calculated loads is not so good (Fig. 9). This may partly be the result of the assumption of moderate rotation in the calculations.

A series of loadings and unloadings was also performed on a UD specimen. The behavior is macroscopically elastic up to strains as large as 2%.

It may be concluded with a good approximation that the glass/epoxy resin UD specimens exhibit a linear elastic behavior under compressive loading in the fiber direction. This also is true for the different laminates tested in this work. In addition anelastic phenomena are not detected in the fiber direction, both for graphite/epoxy resin (Allix *et al.*, 1988) and for glass/epoxy resin composites. It is thus reasonable to suggest that the non-linear behavior observed in compression with graphite/epoxy resin laminates should be ascribed to an intrinsic property of graphite fibers.

Several modes of fracture have been observed, depending on the material (UD or laminate) and on the (M/N) ratio:

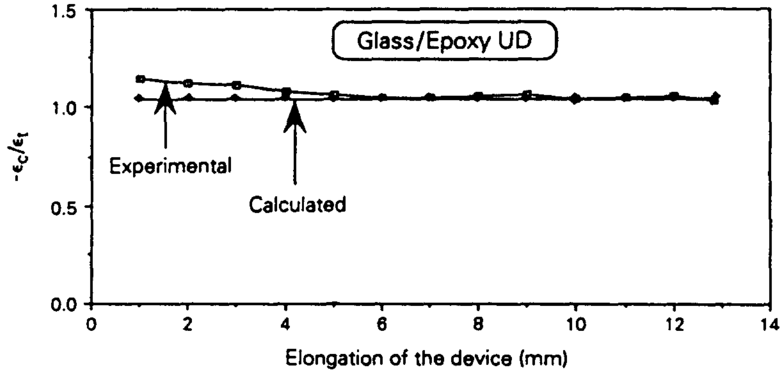

Fig. 8. Experimental and calculated ratios of compressive strain to tensile strain (same experiment as in Fig. 7).

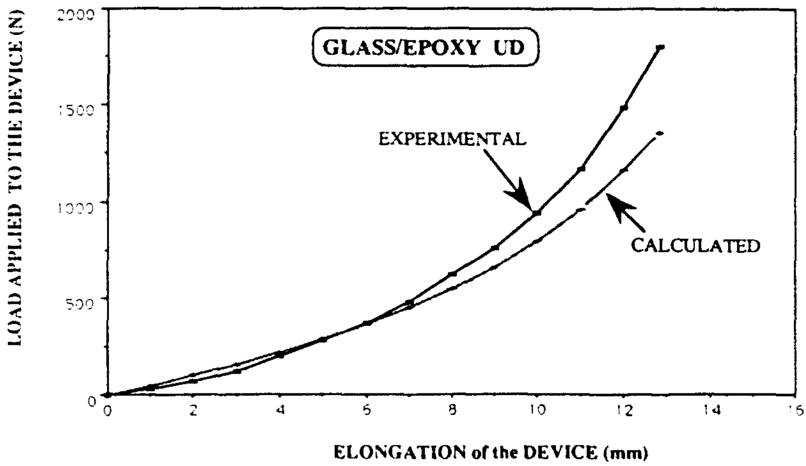

Fig. 9. Experimental and calculated loads (same experiment as in Fig. 7).

Microbuckling has been observed in the form of a decohesion of fibers on the compressed face of the specimens. These decohesions are uniformly distributed on the surface and they propagate in a stable manner. Their wavelength are initially of order of half of the thickness. This phenomenon is noted only in the case of UD specimens and $[0/90/0/90/0]_s$ laminates. In the latter case microbuckling penetrated from the surface into the depth of the specimen and led to the destruction of the external ply. The strain level at which microbuckling occurs is not reproducible, which tends to indicate that initiation may be due to superficial defects.

Delamination is the main failure mode observed when a compressive load is applied. The phenomenon affects the whole width of the specimens, and may be either simple or multiple. It was observed that the number of delaminations increases and that the failure strain decreases as the (M/N) ratio decreases, i.e. when compression predominates. This multiple delamination mode is likely to be the most penalizing failure mode. Actually, the lower failure strains were observed in tests carried out on short specimens under conditions of quasi-pure compression. The failure strains and the modes of failure are reported on Fig. 10 for a UD specimen. The same general trends were obtained on the laminates.

6. CONCLUSION

A more realistic approach to fiber microbuckling in laminated composites under compressive loading has been tentatively proposed in this work. An experimental inves-

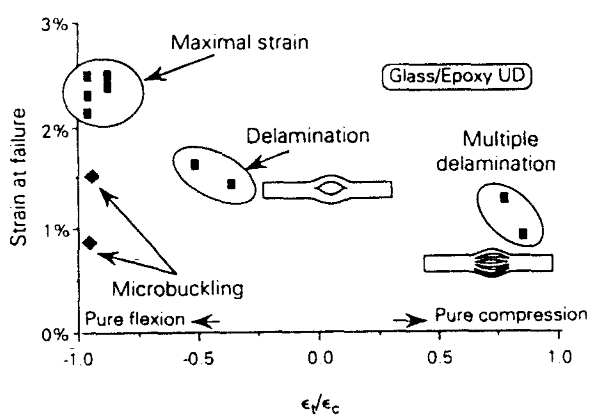

Fig. 10. Failure strains and modes of failure as a function of the ratio of tensile strain to compressive strain. Failure strains are underestimated in quasi-pure flexion, owing to limitations of the device.

tigation of composite behavior under combined flexion and compression has also been performed owing to the use of an original device. The results are summarized as follows.

(1) Thickness effects have been taken into account in a fiber microbuckling model by considering a non-uniform distribution of the deformation of the matrix through the thickness of a ply. The critical microbuckling stresses obtained are much lower than those derived from previous models, and in better agreement with experimental failure strains.
(2) A device has been set up for carrying out flexion–compression tests. Different ratios between the bending moment M and the compressive load N can be obtained by simple changes in the mechanical arrangement.
(3) Microbuckling in the form of detachments of fibers on the face under compression has been observed in flexion on unidirectional glass/epoxy resin composites. On the other hand, delamination is the main mode of failure when a compressive load is applied. The number of delaminations increases and the failure strain decreases as the (M/N) ratio decreases, i.e. when compression predominates.
(4) The elastic behavior of glass/epoxy resin unidirectional composites and laminates has been found to be linear with a good approximation.

Acknowledgements—The authors are indebted to Dr D. Varchon, L. M. A. Besançon, France, for supplying the glass/epoxy resin tapes and for assisting one of them (J.C.G.) in the preparation of the specimens. Vetrotex Company is also acknowledged for kind supply of glass/epoxy resin pre-impregnated strands.

REFERENCES

Allix, O., Girard, F., Ladevèze, P. and Vittecoq, E. (1988). Composite 2D à fibres haute résistance : caractérisation du comportement de compression. JNC6, Paris, pp. 515–526.
Anquez, L. (1990). La rupture en compression des matériaux composites à fibres longues. Note de structure n° 26395 LA/JC, AMD-BA.
Davis, J. G. (1975). Compressive strength of fiber-reinforced composite materials. *ASTM STP* **580**, 364–377.
Grandidier, J.C. and Potier-Ferry, M. (1990) Microflambage des fibres dans un matériau composite à fibres longues. *C. R. Acad. Sci. Paris*, *t.* **310**, Sér. 2, 1–6.
Grandidier, J. C. and Potier-Ferry, M. (1991). Microbuckling and homogenisation for long fiber composites. *ZAMM* **71–4**, 371–374.
Greenwood, J. H. and Rose, P. G. (1974). Compressive behaviour of Kevlar 49 fibres and composites. *J. Mater. Sci.* **9**, pp. 1809–1814.
Greszczuk, L. B. (1975). Microbuckling failure of circular fiber-reinforced composites. *AIAA J.* **13**, 1313–1318.
Greszczuk, L. B. (1982). On failures modes of unidirectional composites under compressive loading. In *Fracture of Composite Materials*. (Edited by G. C. Sih and V. P. Tamuzs), pp. 231–244. Martinus Nijhoff, The Hague.
Hanasaki, S. and Hasegawa, Y. (1974). Compressive strength of unidirectional fibrous composites *J. Composite Mater.* **8**, 306–309.
Harris, C. E. and Lee, J. W. (1988). A micromechanics model for the effective Young's modulus of a piecewise-isotropic laminate with wavy patterns. *J. Composite Mater.* **22**, 717–741.
Kulkarni, S. V., Rice, J. S. and Rosen, B. W. (1975). An investigation of the compressive strength of Kevlar 49/epoxy composite. *Composites* **6**, 217–225.
Rosen, B. W. (1964) Mechanics of composite strengthening. *Fiber Composite Materials*. American Society for Metals.
Sanchez-Palencia E. (1980). Non homogeneous media and vibration theory. *Lecture Notes in Physics*, No. 127. Springer, Berlin.
Schaffers, W. J. (1976). Buckling in fiber-reinforced elastomers. *Textile Res. J.* 502–512.
Steif, P. S. (1987). An exact two-dimensional approach to fiber microbuckling. *Int. J. Solids Structures* **23**, 1235–1246.
Steif, P. S. (1988). A simple model for the compressive failure of weakly bonded fiber reinforced composites. *J. Composite Mater.* **22**, 818–828.
Stevanovic, M. and Nesic, O. (1987). Caractéristiques en compression et défaillance due à la compression des composites carbone/époxyde. *Annales des composites*, 1987/2, pp. 123–139.
Vittecoq, E. (1991). Sur le comportement en compression des composites stratifiés Carbone Epoxy. Thèse, Université Pierre et Marie Curie.